Cell Reports

Article

A recombinant hybrid provides insights into gene regulation, pathogenesis, and tumorigenesis of phytopathogenic smut fungi

Graphical abstract

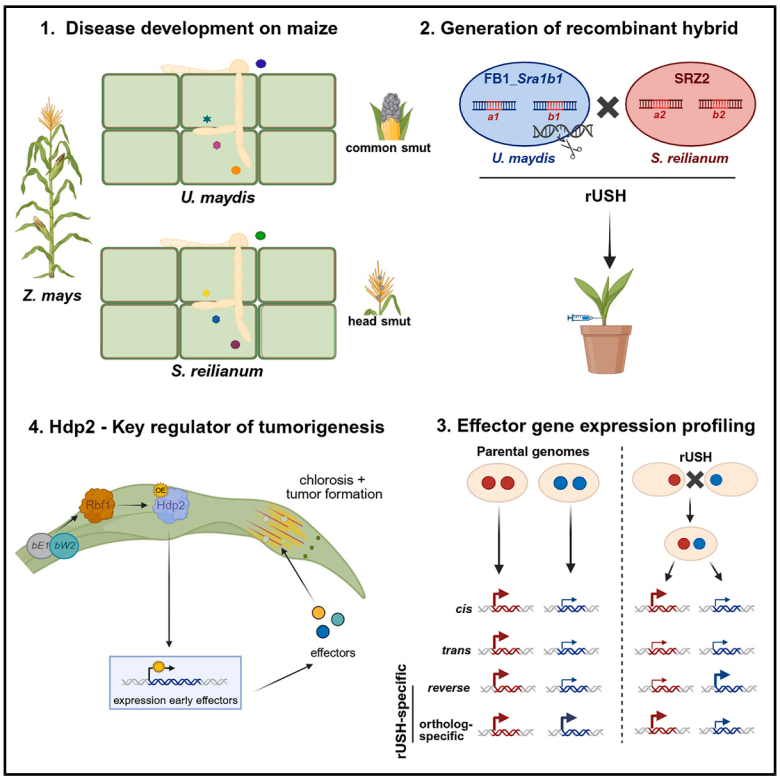

Highlights

- rUSH was generated to elucidate the molecular differences in disease development
- rUSH showed *S. reilianum*-like systemic infection but lacked teliospore formation
- Identification of 253 differentially expressed effector orthologs
- The transcription factor Hdp2 is a central regulator of *U. maydis* tumorigenesis

Authors

Janina Werner, Weiliang Zuo, Tom Winkler, Gunther Doehlemann

Correspondence

g.doehlemann@uni-koeln.de

In brief

A recombinant maize smut hybrid reveals key effectors and a transcription factor driving pathogenic divergence. Werner et al. show that transcriptomics and CRISPR mutagenesis pinpoint novel virulence factors and uncover *Um*Hdp2 as a key regulator of *Ustilago maydis* tumorigenesis.

Werner et al., 2025, Cell Reports *44*, 115772
June 24, 2025
https://doi.org/10.1016/j.celrep.2025.115772

CellPress

Cell Reports

CellPress
OPEN ACCESS

Article

A recombinant hybrid provides insights into gene regulation, pathogenesis, and tumorigenesis of phytopathogenic smut fungi

Janina Werner,[1] Weiliang Zuo,[1] Tom Winkler,[1] and Gunther Doehlemann[1,2,*]
[1]Institute for Plant Sciences and Cluster of Excellence on Plant Sciences (CEPLAS), University of Cologne, Cologne, Germany
[2]Lead contact
*Correspondence: g.doehlemann@uni-koeln.de
https://doi.org/10.1016/j.celrep.2025.115772

SUMMARY

The closely related maize smut fungi *Ustilago maydis* and *Sporisorium reilianum* share genome structures but differ in their pathogenic behavior. *U. maydis* causes local tumors, while *S. reilianum* spreads systemically and affects inflorescences. To investigate the genetic basis of these differences, we generate an interspecific recombinant hybrid (recombinant *U. maydis* x *S. reilianum* hybrid [rUSH]) carrying the *S. reilianum* mating type. rUSH exhibits *in planta* proliferation and an *S. reilianum*-like phenotype, except for teliospore formation. Transcriptome profiling reveals that pathogenicity-related effector orthologs are induced in rUSH but not in a wild-type hybrid control. Comparative transcriptomics identifies 253 differentially expressed one-to-one effector orthologs with *cis*-, *trans*-, and a rUSH-specific phenomenon of *cis/trans*. CRISPR-Cas9 uncovers three novel virulence factors among the rUSH-specific expressed effectors. Ultimately, we pinpoint the transcription factor UmHdp2 as a key regulator of *U. maydis*-induced tumorigenesis. Our findings highlight the utility of a recombinant, interspecific hybrid in unraveling the molecular mechanisms underlying pathogenic differences in closely related fungal pathogens.

INTRODUCTION

Interspecific hybridization events are a phenomenon that gives rise to the emergence of novel fungal pathogens threatening food sustainability. It enables the exchange of fungal genetic material between species through sexual or parasexual mating.[1] Fungal hybrids must navigate potential incompatibilities that arise from the evolution of the parental species.[2] Before two species can successfully hybridize, they need to overcome pre-mating and post-mating barriers.[1] The fitness level of new hybrid species is typically influenced by a number of factors, including genomic incompatibilities of separately evolved alleles, competition with parental species, and the characteristics of the ecological environment in which they are situated.[3] In hybrids, gene expression is significantly influenced by a complex interplay of *cis*-regulatory elements and *trans*-regulatory factors, which are affected by the divergence of the parental species, alterations in chromatin structure, and modifications, as well as RNA interference (RNAi).[4] Nevertheless, due to pre- and post-mating incompatibilities, natural fungal hybrids are rare in nature. However, when such a rare hybridization event occurs between closely related species, it can offer valuable insights into evolutionary traits and host specificity.

Smut fungi infect around 1,500 plant species, mainly including Poaceae. Most smuts infect their host systemically, without evident disease symptoms in the early infection phase, and replace the inflorescences with teliospores. An example of a systemic smut fungus is *Sporisorium reilianum*, which causes head smut in maize (*S. reilianum* f. sp. *zeae*) and sorghum (*S. reilianum* f. sp. *reilianum*). During the early stages of infection, the fungus remains in close proximity to inhabit the vascular bundles, and it displays an endophytic lifestyle.[5] When *S. reilianum* reaches the ear primordia, it can cause the development of multiple female inflorescences and the loss of apical dominance, as well as the formation of sori filled with masses of fungal spores.[5–7] An exception to the typical smut infection process is the model organism *Ustilago maydis*, which causes large tumors locally at all aerial infected parts of maize.[8] The pathogenicity of smut fungi is tightly linked with their sexual cycle, determined by the highly conserved mating-type loci. *U. maydis* and *S. reilianum* comprise a tetrapolar mating-type system, consisting of two unlinked mating-type loci, *a* and *b*. While the *a* locus encodes a pheromone receptor system for the recognition of compatible haploid sporidia, the multiallelic *b* locus encodes for the transcription factors (TFs) bEast (bE) and bWest (bW), which act as heterodimeric key regulators for pathogenicity.[9,10] bE/bW tightly regulate a hierarchical TF network by regulating the master regulator Rbf1 (regulator of b filament)[11] and the downstream TFs Biz1 (b-dependent zinc finger protein 1) and Hdp2 (*homeodomain* transcription factor 2), which are important for the regulation of effector gene expression. The deletion of Biz1 and Hdp2 has been reported to result in a substantial decrease in virulence in *U. maydis*,[12,13] indicating the regulation of the

initial wave of effectors that are crucial for early biotrophic development.[14]

Plant-colonizing microbes secrete a plethora of effector proteins in a spatiotemporal manner to manipulate the host and facilitate host colonization. A genome comparison of *S. reilianum* and *U. maydis* revealed a high degree of synteny, with overall amino acid sequence identities of 74.2% for all predicted proteins and 62% for secreted proteins, suggesting a more rapid evolution of putative effector genes.[15] The genome data of *U. maydis*[16] and *S. reilianum*[15] formed the foundation for the analysis of effector orthologs between the two species. Many effector genes are found in gene clusters. Cluster 19A is the largest cluster identified in both species and contains 24 and 29 secreted effector proteins for *U. maydis* and *S. reilianum*, respectively.[17,18] 19A deletion mutants of *U. maydis* exhibit an inability to induce the formation of large tumors and fail to develop teliospores,[16] in line with the absence of teliospore formation in the 19A1A2 deletion mutant in *S. reilianum*.[7] A number of effectors have already been characterized in *U. maydis* and *S. reilianum*. These have been found to either be functionally conserved, i.e., as evidenced by the effectors See1,[19,20] Pep1,[21] ApB73,[22] and Rsp3,[23] or have different functions, as exemplified by the effectors Tin2 and Sts2,[24,25] respectively. A cross-species transcriptome analysis of *S. reilianum* and *U. maydis* revealed 207 of 336 differentially expressed one-to-one effector orthologs during colonization, suggesting that these genes may contribute to the different disease progressions observed in the two smuts. The findings of this study suggest that the diversification of orthologous effectors in closely related smut fungi can be attributed to two primary factors: transcriptional regulation of effector genes and functional diversification of effector proteins.[5]

It has been shown previously that the haploid *U. maydis* strain 521 (*Uma1b1*) was able to induce filaments with the haploid strain SRZ2 of *S. reilianum*. However, this induction was observed to occur with a lesser degree of effectiveness in comparison to the compatible *U. maydis* mating partner 518 (*Uma2b2*). This finding suggests that interspecific mating also induces pheromone signaling, indicating the presence of similar molecular networks between the species.[26] Nevertheless, the complementation of the bE and bW proteins in *U. maydis* with *S. reilianum* resulted in only partial restoration of tumor formation, which indicates a partial functional conservation of the b proteins.[27] *S. reilianum* and *U. maydis* infect the same host and comprise similar genomes, but no natural hybridization events have been reported so far. However, under laboratory conditions, a fungal hybrid of the two smut fungi, *Ustilago bromivora* infecting *Brachypodium* spp. and *Ustilago hordei* infecting barley, is able to infect *Brachypodium* spp., while *U. hordei* alone was unable.[28] Moreover, a fungal hybrid of *S. reilianum* and *U. maydis* was employed to investigate their differences in the disease symptoms. However, after successful formation of a dikaryotic hyphae, a lack of fungal proliferation and a delayed development of disease symptoms were observed for the hybrid compared to the parental species.[29] Therefore, we hypothesized that the utilization of the mating-type system of a single species to generate a recombinant interspecific hybrid of *S. reilianum* and *U. maydis* may enhance the fitness of the hybrid *in planta*, promote increased compatibility of downstream processes, and offer insights into the differential progression of diseases.

In this study, we generated a *U. maydis* strain harboring the *a* and *b* mating loci from *S. reilianum* and developed a recombinant *U. maydis* x *S. reilianum* hybrid (rUSH) as a tool to elucidate differences in the disease development of the two pathogens. rUSH propagated during infection and led to a disease symptom that bears resemblance to *S. reilianum*. Using RNA sequencing (RNA-seq), we identified a total of 253 effector orthologs changing their expression patterns in rUSH compared to those between parental species, which led to the identification of novel *U. maydis* and *S. reilianum* virulence factors, contributing to the different disease phenotypes. This identified distinct expression patterns of effector genes: *cis*-, *trans*-, and rUSH-specific *cis/trans* expression patterns. Ultimately, overexpressing the TF *Um*Hdp2 was found to enable rUSH to induce maize tumorigenesis, which is linked with the upregulation of a set of 41 *U. maydis* effector genes.

RESULTS

Generation of the recombinant smut hybrid rUSH

In a two-step sequential transformation, we replaced the mating-type loci *Uma1* and *Umb1* in the *U. maydis* haploid wild-type (WT) strain FB1 with *S. reilianum Sra1* and *Srb1*. Using CRISPR-assisted homologous recombination, this resulted in strain FB1_*Sra1b1*. To generate an interspecific hybrid, FB1_*Sra1b1* was used together with the mating-compatible partner of *S. reilianum*, SRZ2 (*Sra2b2*), and the resulting hybrid was further named rUSH (Figure 1A). We further exchanged *Sra1* and *Srb1* mating-type loci in SRZ1 against *Uma1* and *Umb1* (SRZ1_*Uma1b1*; Figures S1A and S1B) and used them together with FB2 (rSUH) in infection assays. In contrast to rUSH, rSUH did not reveal a viable hybrid when infected with the haploid *U. maydis* strain FB2. Biomass quantification and WGA-AF488 staining of rSUH-infected maize leaves were performed, which revealed no increase or clump formation, respectively (Figures S1C and S1D). This is in line with the mating assays, where 521 (*Uma1b1*) xSRZ2 was able to induce filament formation, while SRZ1x518 (*Uma2b2*) was not.[26] Consequently, rUSH (FB1_*Sra1b1*xSRZ2) was employed for the subsequent analysis of this study.

rUSH proliferates *in planta* and reveals an *S. reilianum*-like phenotype

To investigate the viability of rUSH, we tested its ability to form filaments. Therefore, liquid culture of rUSH was dropped on PDA plates supplemented with activated charcoal, which revealed a typical fuzzy filament[30] (Figure 1B). To confirm the formation of a dikaryotic filament, mCherry and GFP-tagged histone1 (H1) were integrated into the *ip* locus of FB1_*Sra1b1* and SRZ2 (Figure 1C), respectively. These strains resulted in rUSH with one red and one green fluorescent nucleus each, deriving from *U. maydis* and *S. reilianum*, respectively. Confocal microscopy of the filament from PDA + charcoal (Figure 1F) and *in planta* 2 days post-infection (dpi) verified the presence of one mCherry- and one GFP-labeled nucleus each in one filament cell (Figure 1D). As a control, an FB1_*Sra1b1* strain with a cytosolic (pro^{actin}) mCherry was used together with SRZ2 (Figure 1E).

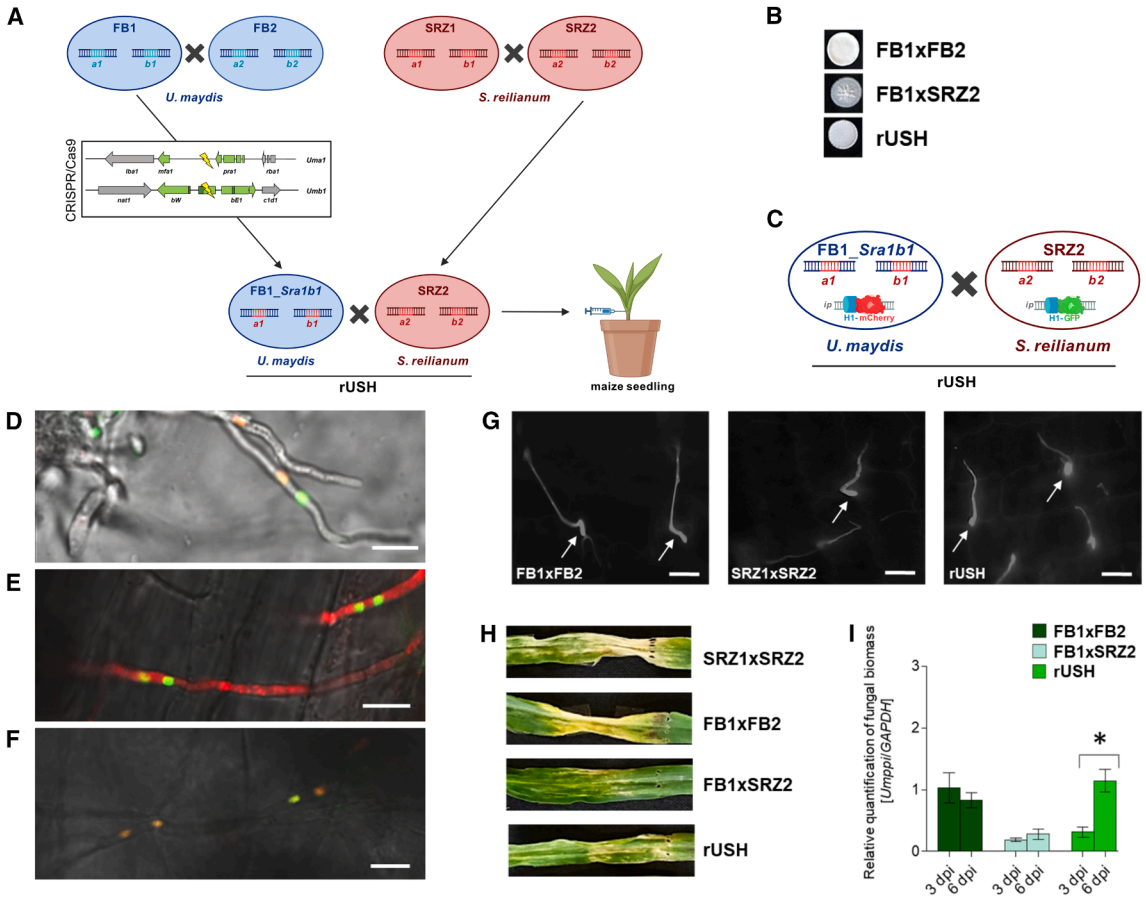

Figure 1. *In planta* proliferation of the recombinant *U. maydis* x *S. reilianum* hybrid

(A) Generation of recombinant *U. maydis* x *S. reilianum* hybrid (rUSH). The mating loci *a1* and *b1* of *U. maydis* FB1 strain were replaced by using CRISPR-Cas9-mediated homologous recombination to generate a mutant containing the *S. reilianum* mating loci *Sra1b1* (FB1_*Sra1b1*). This strain was mixed with the mating-compatible *S. reilianum* strain (SRZ2) to generate rUSH for infection.

(B) The mix of different mating strains (FB1xFB2, FB1xSRZ2, and FB1_*Sra1b1*xSRZ2 [rUSH]) on PD-charcoal plate.

(C) mCherry and GFP-tagged histone1 were integrated into *ip* locus of FB1_*Sra1b1* and SRZ2, respectively, to visualize the source of the nuclei.

(D) Confocal microscopy of FB1_*Sra1b1*_H1_mCherryxSRZ2_H1_GFP on activated charcoal.

(E) Confocal microscopy of 2 dpi maize leaf infected with FB1_*Sra1b1*_mCherry(cytosolic)xSRZ2_H1_GFP.

(F) Confocal microscopy of 2 dpi maize leaf infected with FB1_*Sra1b1*_H1_mCherryxSRZ2_H1_GFP.

(G) Calcofluor white staining of maize leaves (20–22 hpi) shows the formation of the appressoria-like structures (indicated in white arrows).

(H) Phenotype (6 dpi) of SRZ1xSRZ2-, FB1xFB2-, and rUSH-infected maize leaves.

(I) Quantification of fungal biomass at 3 and 6 dpi. Housekeeping genes *ZmGAPDH* and *Umppi* were used for quantification.

Data are represented as mean ± SEM. Significance was calculated by Students t test: $^{*}p < 0.05$. Scale bars (D–G): 10 μM.

Following the life cycle of *U. maydis* further, we investigated the ability of rUSH to form penetration hyphae. Calcofluor white staining of 22 hpi (h post-infection) infected maize seedlings resulted in an observation of appressoria-like structures for *U. maydis*, *S. reilianum*, and rUSH (Figure 1G). In summary, rUSH was found to be capable of forming dikaryotic filaments and appressoria-like structures.

Next, the infection phenotypes of rUSH were assessed in comparison to *U. maydis* and *S. reilianum*. Maize seedlings (cultivar: Golden Bantam) infected with rUSH, *U. maydis*, and *S. reilianum* were assessed at 6 dpi (Figure 1H). Seedling infections were monitored at 3 weeks post-infection (wpi) and in 7 wpi maize plants (cultivar: Gaspe Flint), respectively (Figure 2). Interestingly, rUSH caused an *S. reilianum*-like phenotype with the induction of chlorotic and necrotic spots at 6 dpi, and at 7 wpi, a few infected plants showed leafy tassels and ears (Figure 2). In general, the rUSH phenotypes were similar but milder compared to those of *S. reilianum* in all infection experiments performed in this study. We measured the relative fungal biomass of maize leaves infected with FB1xFB2, FB1xSRZ2, and rUSH at 3 and 6 dpi. rUSH revealed an increase in biomass between 3 and 6 dpi, in contrast to the control FB1xSRZ2 (Figure 1J). To gain further insight into the underlying gene expression patterns, we conducted an RNA-seq experiment at 3 dpi. In the WT FB1xSRZ2 hybrid, expression of known crucial effector genes, including *cmu1*,[31] *pit2*,[32,33] *stp2*, *stp3*, *stp5*, and *stp6*,[34] was not detected (Figure S3B; Table S1), which most likely explains the inability to further proliferate in the host tissue.

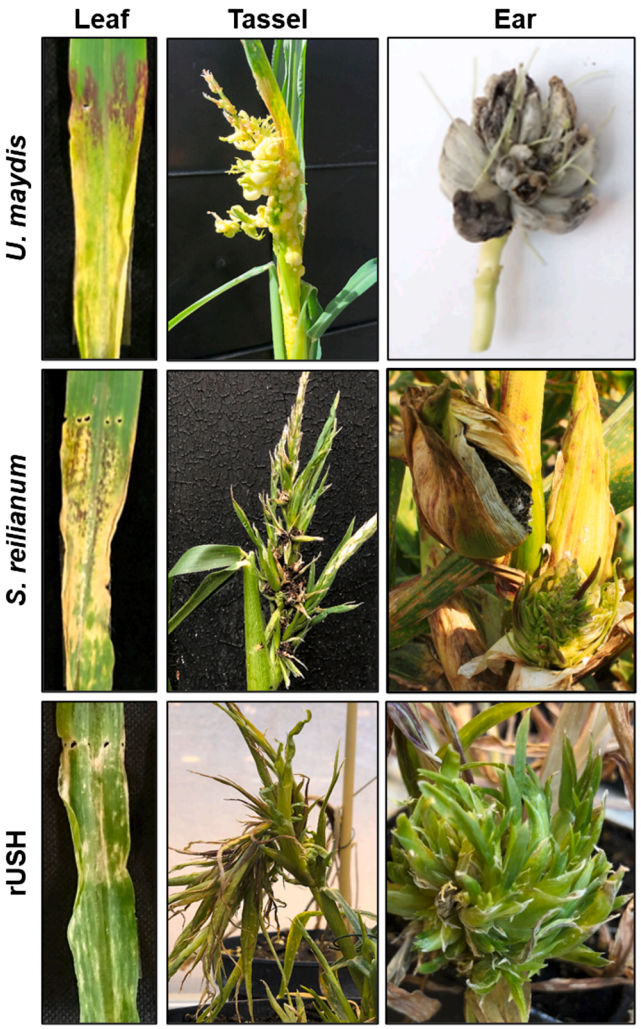

Figure 2. rUSH shows an *S. reilianum*-like phenotype in different maize organs

Phenotype of *U. maydis* wild-type FB1xFB2, *S. reilianum* wild-type SRZ1xSRZ2, and rUSH at 6 dpi (leaf), 3 wpi *U. maydis* (tassel), or 7 wpi for *S. reilianum* (tassel, ear) and *U. maydis* (ear).

In contrast, we observed significant induction of 119 *U. maydis* and 294 *S reilianum* effector one-to-one orthologs[5] in rUSH (Figure S4). This effector gene induction in rUSH can be expected to result in an efficient suppression of plant defense responses. Consequently, the recombinant hybrid was able to maintain the biotrophic interaction, which is reflected by the increasing fungal biomass from 3 to 6 dpi (Figure 1J). Together, these results suggest that the reconstruction of a single species' mating-type system leads to a stable and compatible downstream signaling in the interspecies hybrid, and consequently, the hybrid is able to colonize the host.

S. reilianum effector gene orthologs are dominantly expressed in rUSH

To understand how effector ortholog expression contributes to the observed *S. reilianum*-like phenotype, RT-qPCR of two effector genes, *pit2* and *see1*,[20,32] was performed for *S. reilianum*-, *U. maydis*-, and rUSH-infected maize seedlings at 20–22 hpi, 3 dpi, and 6 dpi (Figure S2A). For the *U. maydis* orthologs *Umpit2* and *Umsee1*, the expression levels were significantly reduced in rUSH at 6 dpi compared to FB1xFB2. In contrast, the *S. reilianum* orthologs *Srpit2* and *Srsee1* were significantly more highly expressed in rUSH at 6 dpi compared to *S. reilianum*, indicating an opposite expression pattern of these orthologs in rUSH (Figure S2A). RT-qPCR results suggested generally lower expression of *U. maydis* orthologs compared to the *S. reilianum* genes. To test whether the RNAi machinery in *S. reilianum*, which is absent in *U. maydis*,[15] is associated with this downregulation of the *U. maydis* orthologs in rUSH, a dicer (*sr16838*) knockout was generated in the SRZ2 background (Figure S2B). However, when the gene expression levels of *Umsee1*, *Umtin2*, and *Umnlt1* were measured in rUSH and two independent rUSH dicer deletion strains, no change in expression levels was observed, suggesting that the observed downregulation effect of *U. maydis* orthologs is not caused by RNAi (Figure S2D).

Next, we tested whether ortholog-specific suppression of the *U. maydis* gene expression takes place. To this, we used the effector gene *Umtin2*, which had been shown to induce maize anthocyanin formation.[35] Moreover, its ortholog, SrTin2, can complement neither the virulence nor the anthocyanin formation of the mutant Δ*Umtin2*.[24] Thus, the observation that rUSH infection did not induce anthocyanin formation is in accordance with the ortholog-specific gene expressions of *Srtin2* in rUSH (Figures 3A and 3B). To investigate whether locus-specific inhibition of *Umtin2* expression takes place in *U. maydis*, we used the promoter of *Srtin2*, pro^{Srtin2}, to control the expression of *Umtin2* in the native *Umtin2* locus of FB1_*Sra1b1* (Figure 3C). As a control, we replaced the coding sequence of *Srtin2* with *Umtin2* in its native locus in SRZ2 (Figure 3D) using CRISPR-mediated knockin. In an infection assay, FB1_*Sra1b1*_pro^{Srtin2}_*Umtin2* x SRZ2 and FB1_*Sra1b1* x SRZ2_pro^{Srtin2}_*Umtin2* induced anthocyanin formation, which is absent in rUSH (Figure 3D). This demonstrates that the induction of *Umtin2* in rUSH can be restored by maintaining the *cis*-regulatory element of the promoter of *Srtin2*, which also excludes locus-specific suppression of the *U. maydis* ortholog. However, at present, regulatory differences between *Umtin2* and *Srtin2* are far from being fully understood on a genome-wide scale, and this might involve either variations in the *cis*-regulatory elements or different TFs between the species.

Transcriptome analysis reveals distinct expression patterns of one-to-one effector genes in rUSH

For genome-wide profiling of effector ortholog expression in rUSH, RNA-seq of *U. maydis* (FB1xFB2), *S. reilianum* (SRZ1xSRZ2), and rUSH was conducted at 20–22 hpi (penetration stage), 3 dpi (early biotrophic development), and 6 dpi (*U. maydis* tumorigenesis) (Figure 4A; Table S2). In line with previous findings, where relative reads were compared between species,[5] we obtained significantly more reads for *S. reilianum* at 3 and 6 dpi than for *U. maydis* (Figure 4B). In rUSH, the read contribution from each fungal species was comparable at 20 hpi and 3 dpi, and slightly more reads

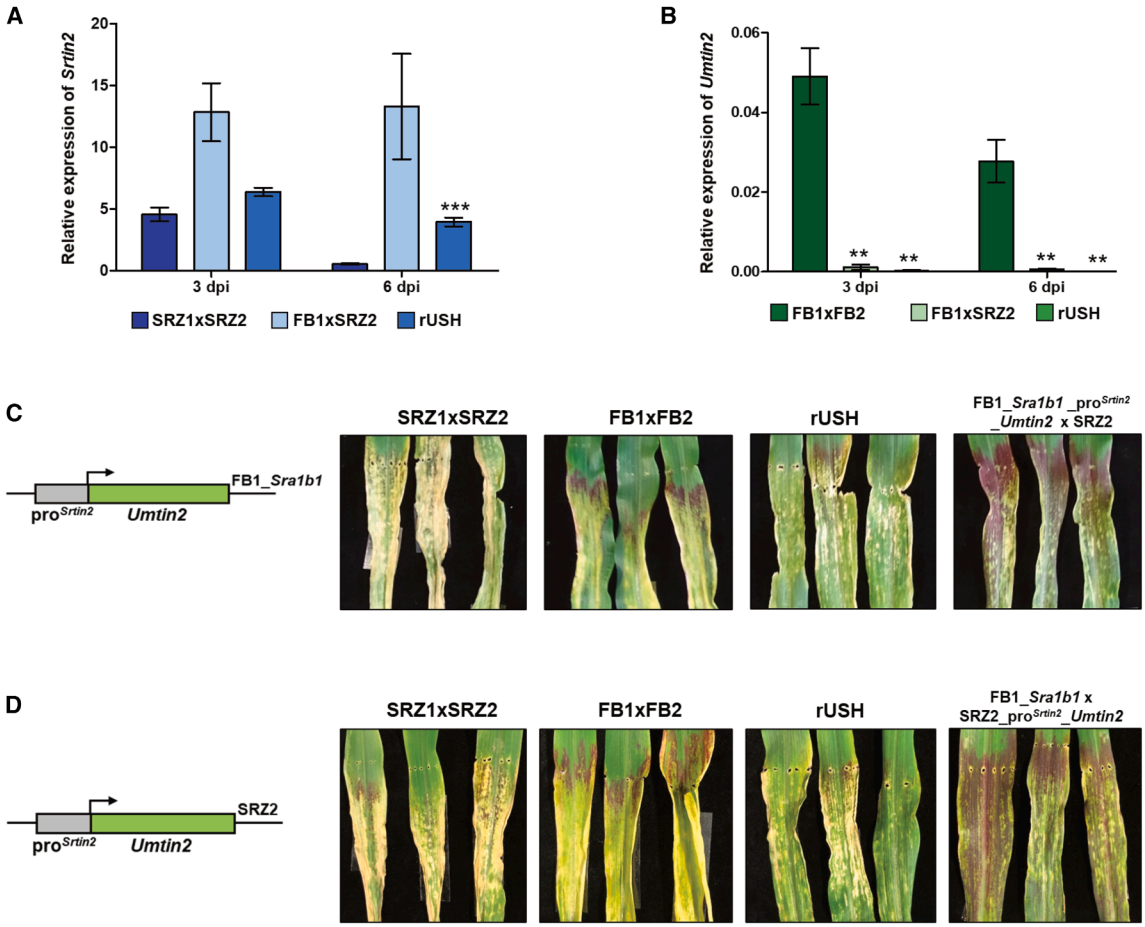

Figure 3. The differential regulation of *Umtin2* ortholog in rUSH is caused by *cis*-regulation in the promoter

(A) RT-qPCR detection of *Srtin2* expression in SRZ1xSRZ2, FB1xSRZ2, and rUSH at 3 and 6 dpi. *Srppi* is used for normalization.

(B) Relative expression of *Umtin2* in FB1xFB2, FB1xSRZ2, and rUSH. *Umppi* is used for normalization.

(C and D) Phenotype assessment of rUSH: pro^{Srtin2} controlling *Umtin2* in FB1_*Sra1b1* and (C) pro^{Srtin2} controlling *Umtin2* in *S. reilianum* SRZ2. (D) Photos of typical phenotypes of different infections at 6 dpi.

Data are represented as mean ± SEM. Error bars (standard deviation) were calculated from three biological replicates. Significant differences were calculated based on Student's t test: $^{**}p < 0.01$ and $^{***}p < 0.001$.

were obtained from *U. maydis* at 6 dpi (Figure 4C). Epidermal penetration and initiation of the biotrophic development (20–22 hpi) are similar in both pathogens.[5] During leaf colonization, the development of the two pathogens gets increasingly distinct, particularly at 6 dpi, when only *U. maydis*, but not *S. reilianum*, is inducing tumor formation. This corresponds with an increasing differential expression of effector orthologs over time: we identified 75 differentially expressed one-to-one effector genes ($\log_2$ fold change [$\log_2$FC] > 1 or < −1; $p < 0.05$) at 20–22 hpi, 114 at 3 dpi, and 152 at 6 dpi (Figures 4D and 4E). Based on the expression profiles of the one-to-one orthologs between the WT and rUSH, ortholog clustering was performed, which revealed 8 clusters with distinct expression patterns (Figure 4F). After examining the expression levels of one-to-one orthologs in *U. maydis*, *S. reilianum*, and rUSH, we identified three distinct expression patterns, *cis* (84), *trans* (61), and rUSH-specific expression (108) (Table S3), and these patterns can be associated with the different clusters observed. *Cis*-expressed effector genes reflect the same trend of differential expression between *U. maydis* and *S. reilianum* and within rUSH, indicating that *cis*-regulatory elements in the promoter region contributed to the differential expression. *Trans*-regulated expression indicates the differential expression between *U. maydis* and *S. reilianum*, which is gone in rUSH, influenced by the presence/absence of a TF or the different threshold of TF expression. Lastly, the rUSH-specific expression revealed two different observations: reverse expression (58), in which one ortholog shows a dominant expression in either *U. maydis* or *S. reilianum*, while the opposite ortholog has higher expression in rUSH, and ortholog-specific expression (50), where only one ortholog changes the expression in rUSH compared to *U. maydis* and *S. reilianum* (Figure 5A). Within the rUSH-specific reverse expression pattern, previously characterized effector genes are included, i.e., *pit2*, *tip1*, *tip2*, and *tip4-6*,[32,36,37] which are known to contribute to *U. maydis* virulence in maize leaves.

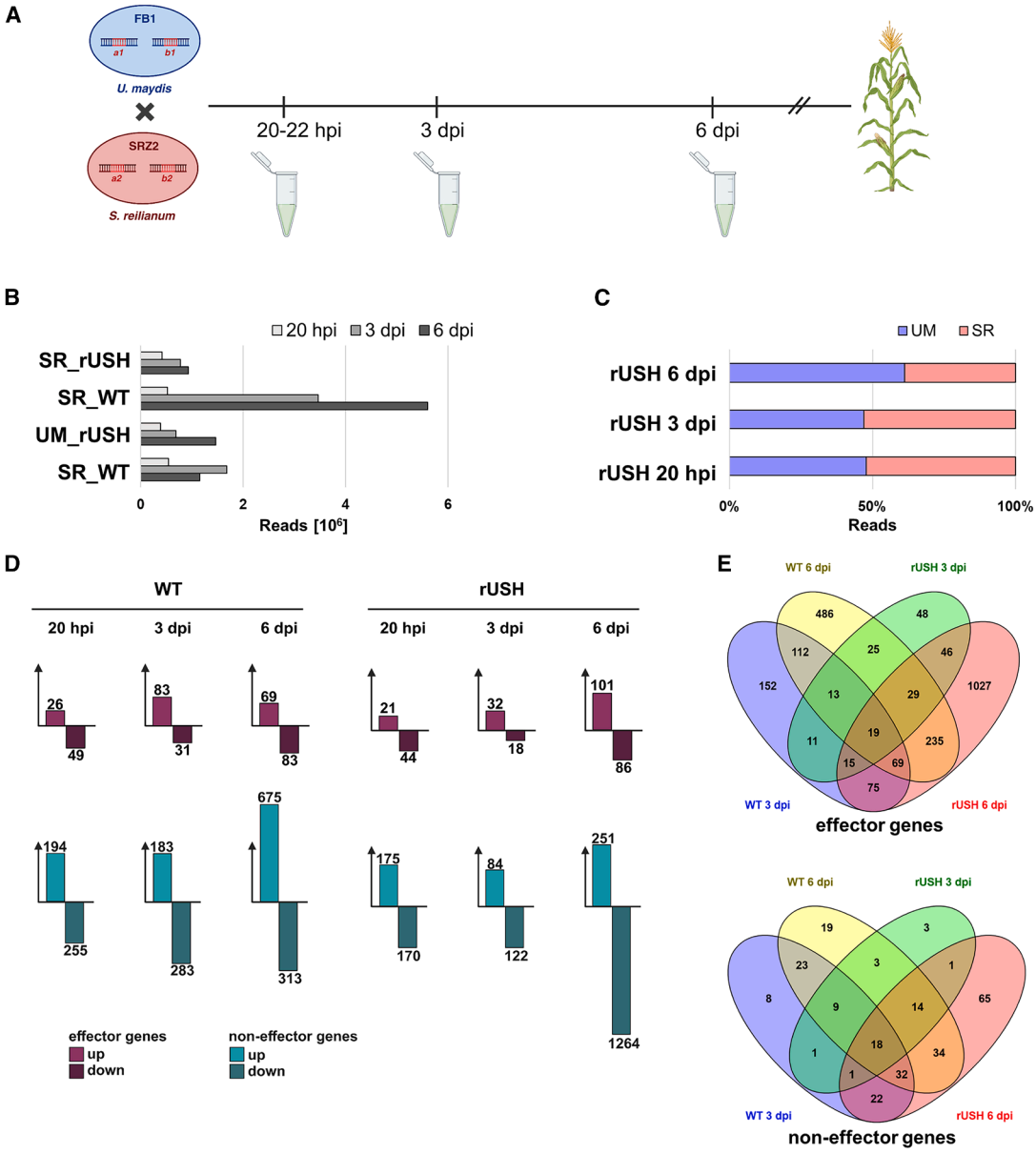

Figure 4. RNA-seq of rUSH compared to FB1xFB2 and SRZ1xSRZ2 at 20–22 hpi, 3 dpi, and 6 dpi

(A) Time points of RNA-seq sampling. At 20–22 hpi, fungal material on the plant surface was enriched using liquid latex. At 3 and 6 dpi, 4 cm of plant material was used for the extraction of total RNA.

(B) Total reads were obtained from each species at 20 hpi, 3 dpi, and 6 dpi.

(C) Relative reads from *U. maydis* and *S. reilianum* in rUSH at 20 hpi, 3 dpi, and 6 dpi.

(D) Bar plots show the number of differentially expressed one-to-one effector orthologs and non-effector orthologs[5] between *S. reilianum* and *U. maydis* (WT) and between *S. reilianum* and *U. maydis* within rUSH.

(E) Venn diagrams show the overlap of effector orthologs and non-effector orthologs at 3 and 6 dpi in FB1xFB2 (WT) and rUSH.

(F) Heatmap shows the $\log_2$ fold change ($\log_2$FC) between *U. maydis* and *S. reilianum* orthologs between WT or within rUSH. Ortholog clustering was performed based on the expression profiles between WT and rUSH using one minus Pearson correlation and K-means clustering.

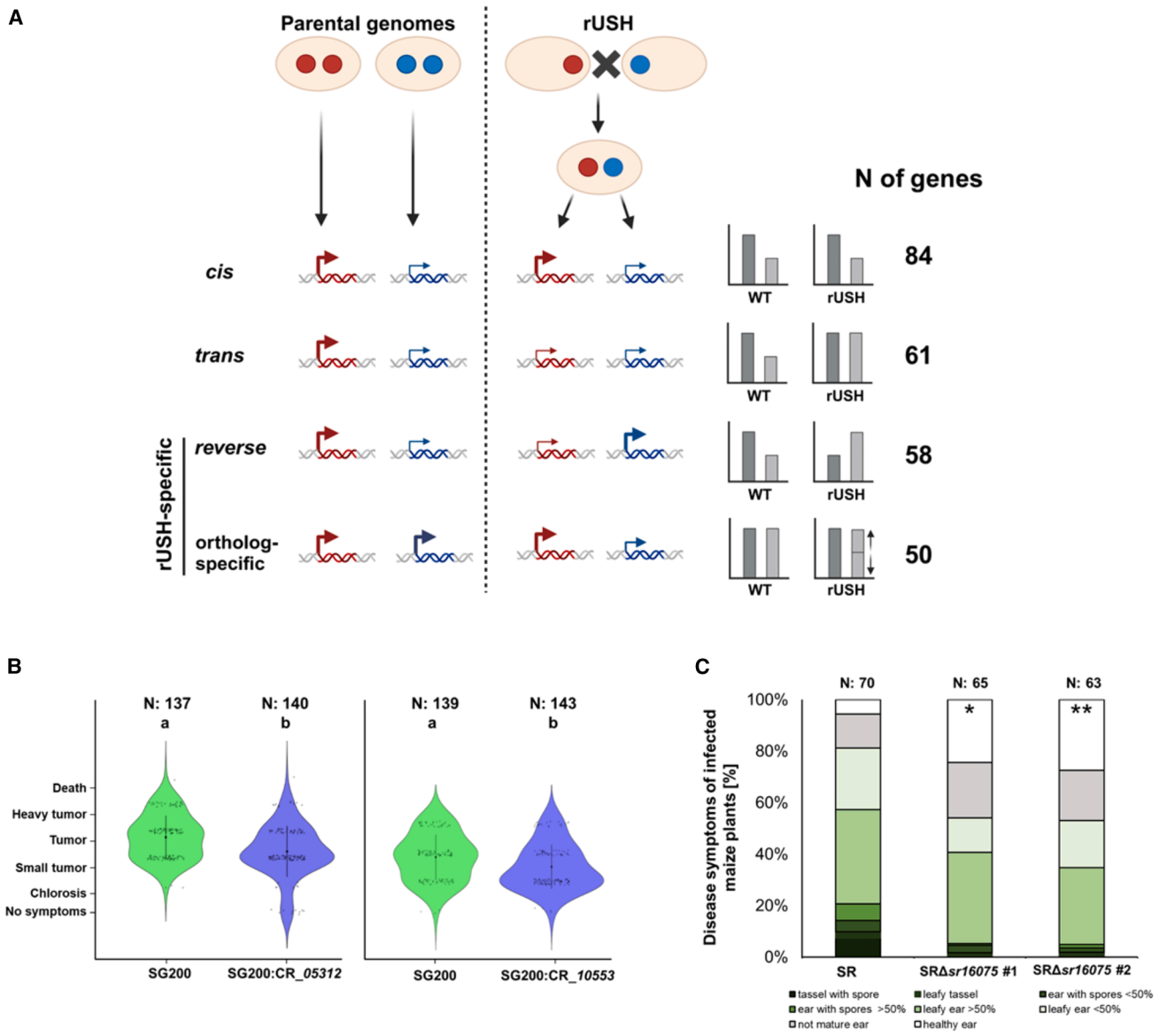

Figure 5. Effector orthologs in rUSH reveal novel expression patterns compared to wild type

(A) Expression patterns of differentially expressed one-to-one effector orthologs in rUSH. Effector orthologs between the wild-type *U. maydis* and *S. reilianum* are differentially expressed. (1) *Cis*: retains the same expression in rUSH, (2) *trans*: exhibits an equal expression between the two orthologs within rUSH, (3) reverse expression: shows the opposite expression in rUSH, and (4) ortholog-specific expression: only one ortholog changes the expression within rUSH. The effector gene expression was calculated by dividing the *S. reilianum* transcripts per million (TPM) by *U. maydis* TPM of the wild types FB1xFB2 and SRZ1xSRZ2 (SR_WT/UM_WT) as well as within rUSH (SR_rUSH/UM_rUSH).

(B) Infection assay of SG200, SG200:CR_UMAG_05312, and SG200:CR_UMAG_10553 at 12 dpi. 7-day-old maize seedlings were infected with SG200 and mutant strains. Data are represented as mean ± SEM. Significant differences were calculated based on Tukey's two-way ANOVA.

(C) Infection assay of early flowering maize cultivar Gaspe Flint with *S. reilianum* wild-type SR (SRZ1xSRZ2) and two independent mutants of *sr16075* (SRZ1Δ*sr16075*xSRZ2Δ*sr16075*: SRΔ*sr16075* #1 and #2). 7-day-old maize seedlings were infected with a final OD of 1 of the mating-type combinations. Disease symptoms were scored 8 wpi as described previously (Ghareeb et al.[18]).

Data are represented as mean ± SEM. Significant differences were calculated based on Student's t test: $^{*}p < 0.05$ and $^{**}p < 0.01$.

Effector genes with rUSH-specific expression encode virulence factors

Effector genes that are typically highly induced during *U. maydis* infection were significantly downregulated in rUSH (Table S4). This finding is of particular interest with regard to the absence of tumor induction by rUSH. In line with this *S. reilianum*-like phenotype, we hypothesized that those *U. maydis* effector genes that are downregulated in rUSH are most likely linked to tumorigenesis. To follow this assumption and to identify effector genes that contribute to *U. maydis*-induced tumorigenesis, we set a

stringent cutoff of at least 5-fold higher expression in the *U. maydis* WT compared to rUSH. The resulting candidate list of 14 tumorigenic effector candidate genes (Table S5) includes effector genes that have already been functionally characterized, including the *U. maydis* virulence factors Pep1, Sts2, Tip6, and Tip7.[25,37–39] To identify novel virulence factors, six candidate genes that had not been investigated in previous studies were selected to further functional characterization. CRISPR-Cas9 (CR) frameshift mutants were generated in *U. maydis*, and the resulting mutant strains were tested in maize infection assays. Strikingly, two of the selected candidate genes (*UMAG_05312* and *UMAG_10553*) were identified as virulence factors, i.e., the respective mutant strains showed significantly reduced tumorigenesis compared to the progenitor strain SG200 (Figure 5B). This result confirms the hypothesis that reverse-expressed effectors with downregulation in rUSH are involved in tumor formation.

In a complementary approach, we also checked the expression levels of *S. reilianum* effector genes in rUSH compared to *S. reilianum*. This revealed 108 *S reilianum* effector genes in rUSH with at least 2-fold higher expression levels compared to *S. reilianum* (Table S6). Using CR mutagenesis, we generated compatible *S. reilianum* knockout strains of the most highly expressed effector candidate, *sr16075*, in our list. Maize infection assays revealed a reduction of virulence with a significant increase in healthy ears compared to the *S. reilianum* WT at 7 wpi (Figure 5C). Thus, the mutation of effector genes with a rUSH-specific expression pattern in rUSH identified novel virulence factors in both *U. maydis* and *S. reilianum.*

The TF Hdp2 regulates tumorigenic effector genes

The differential expression patterns of *U. maydis*/*S. reilianum* WT strains and rUSH might be caused either by different *cis*-regulatory elements in the promoter region of the effector genes or by the presence/absence or a certain threshold of a TF. To identify TFs implicated in the transcriptional regulation of differential gene expression and, consequently, the different disease progression of *U. maydis* and *S. reilianum*, we sought out one-to-one non-effector genes with a predicted DNA-binding function. This led to the identification of 78 candidate TFs (Table S7). We evaluated the candidates with a focus on TFs with lower *U. maydis* ortholog expression in rUSH compared to the WT. Furthermore, we selected reverse-expressed TF candidates with a high expression of the *S. reilianum* one-to-one ortholog in rUSH, while in the *U. maydis*-*S. reilianum* comparison, the *U. maydis* ortholog is more highly expressed. Based on these parameters, five candidates were selected to generate CR frameshift mutants in the *U. maydis* background for subsequent pathogenicity assays (Figure S4F). However, none of the five candidate genes exhibited a role in *U. maydis* virulence (Figures S4A–S4E). We therefore compared the expression patterns of known, pathogenicity-related *U. maydis* TFs in rUSH with their expression in *U. maydis.* Here, we observed an overall higher expression of their *S. reilianum* one-to-one orthologs in rUSH (Figure S4G). Based on this observation, we hypothesized that this low expression of *U. maydis* TF orthologs might be functionally linked with the *S. reilianum*-like phenotype of rUSH. If true, one would therefore expect that an overexpression of these TFs in rUSH might shift the pathogenic behavior of the hybrid toward *U. maydis*, i.e., the formation of leaf tumors. Support of this hypothesis is also given by a previous study, where overexpression of *Umrbf1* and *Umhdp2* in 521xSRZ2 revealed the induction of small tumors in a rare event.[29] We therefore overexpressed the *U. maydis* TFs *Umrbf1*, *Umnlt1*, *Umfox1*, *Umros1*, and *Umhdp2*[11,13,40–42] in rUSH, using the promoter of *U. maydis* effector gene *cmu1* (pro^{Umcmu1}),[31] which confers high expression in *U. maydis* throughout biotrophic development.[31,43] The overexpression of *Umrbf1*, *Umnlt1*, *Umfox1*, and *Umros1* in rUSH did not cause a significant change in rUSH infection (Figure S4H). However, when maize leaves were infected with rUSH overexpressing *Umhdp2*, tumor formation locally at sites of infection was observed (Figure 6A) in all tested plants, which strikingly resembled the typical disease phenotype caused by *U. maydis*.

Thus, genes being induced by *Um*Hdp2 in rUSH are most likely to be functionally linked with tumorigenesis. To identify the genes, an RNA-seq experiment was conducted, comparing rUSH_OE_*Umhdp2* and rUSH. This identified 41 *U. maydis* effector genes being upregulated by *Um*Hdp2, including 13 and 5 genes that reside in the effector clusters 19A and 6A,[16] respectively. Additionally, 12 non-effector genes were upregulated in rUSH_OE_*Umhdp2* (Figure 6B). In line with the observed tumor formation, we identified 1,145 upregulated maize genes (Figure 6C; Table S9) in rUSH_OE_*Umhdp2* vs. rUSH. Here, genes associated with metabolic/catabolic processes and cell cycle control were enriched (Table S10). These processes have previously been found to be associated with *U. maydis*-induced tumor induction[20,44] Within the genes enriched in cell cycle processes, 14 genes were associated with the regulation of mitotic nuclear division, 18 with the regulation of mitotic cycle, and 16 with cell cycle transition (Figure 6D). Strikingly, this also included the leaf developmental markers *ZmGIF1* and *ZmSHR1*, which we recently found to be induced by the tumor-inducing effector Sts2.[25] The identification of *ZmGIF1* and *ZmSHR1* in two independent RNA-seq analyses as potential targets of *U. maydis* in maize, involved in tumorigenesis (this study),[25] renders them promising candidates for investigating the underlying mechanisms of *U. maydis*-induced leaf tumor development in the future.

DISCUSSION

U. maydis and *S. reilianum* are closely related pathogen species that infect the same host plant, but they differ fundamentally in their infection styles. Apart from two characterized tumorigenic effectors, See1 and Sts2,[20,25] the genetic basis of *U. maydis* tumor formation remains largely unknown. In this study, we generated a rUSH as a tool to investigate the different disease developments of the two pathogens, in particular with regard to tumorigenesis. rUSH successfully colonized maize leaves and inflorescences and displayed an *S. reilianum*-like phenotype. Transcriptome analysis of *U. maydis*, *S. reilianum*, and rUSH identified the phenomenon of a rUSH-specific expression of effector orthologs, which revealed novel virulence factors of both pathogens and identified *Um*Hdp2 as a key transcriptional regulator for the induction of *U. maydis*' tumorigenesis.

Previous approaches to generate smut hybrids between *U. maydis* and *S. reilianum* without altering the mating-type loci,

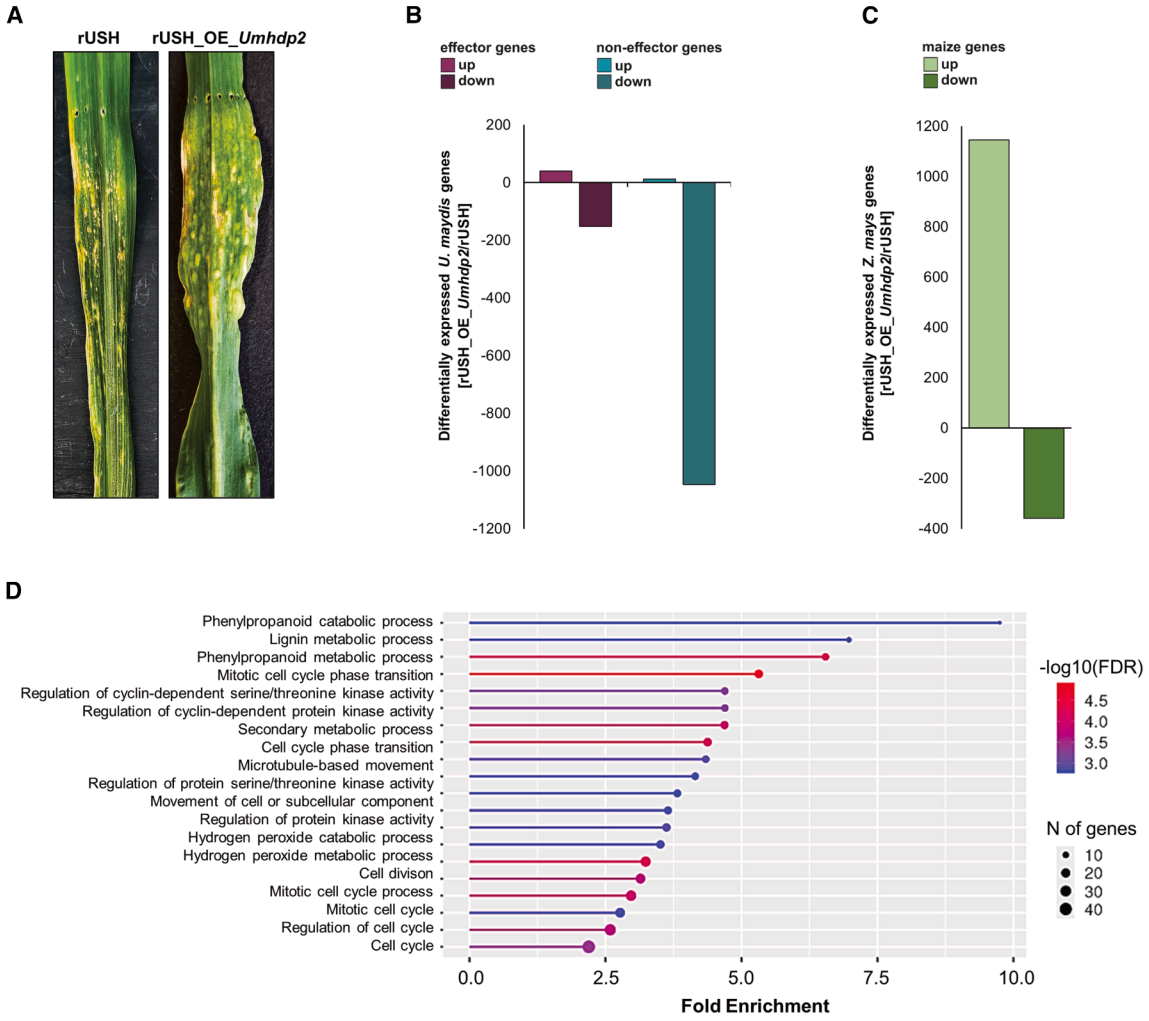

Figure 6. Overexpression of the transcription factor *Umhdp2* leads to tumor formation on rUSH-infected maize leaves

(A) Phenotype of rUSH and rUSH_OE_*Umhdp2* at 6 dpi.

(B) Differentially expressed *U. maydis* effector genes and non-effector genes.

(C) Differentially expressed maize genes in rUSH_OE_*Umhdp2* in comparison to rUSH (rUSH_OE_*Umhdp2*/rUSH).

(D) GO Enrichment analysis of 1,145 upregulated maize genes in rUSH_OE_*Umhdp2* compared to rUSH (ShinyGO 0.66).

such as protoplast fusion[45] or the laboratory hybrid 521xSRZ2,[29] resulted in valuable insights but were limited in their pathogenic development. The high conservation of the mating-type systems between *U. maydis* and *S. reilianum* eliminated pre-mating barriers, facilitating successful mating and the formation of dikaryotic hyphae. Comparative genetics, along with sexual compatibility tests conducted by Kellner et al.,[26] showed the compatibility between haploid strains of *U. maydis* and *S. reilianum*. In accordance with our observations on rUSH, only *U. maydis* 521 (*Uma1b1*) was observed to induce filaments with the second mating partner of *S. reilianum* (SRZ2), and not vice versa.[26]

Our transcriptome analysis revealed a lack of expression of key effector genes in WT FB1xSRZ2 hybrids, which is in line with the attenuated host colonization of 521xSRZ2[29] and FB1xSRZ2 (this study). This reflects the general fitness deficits in the natural combination of interspecies mating types, which is overcome by the recombinant mating-type loci in rUSH. However, in our hands, rUSH was unable to produce teliospores, which are necessary for further sexual reproduction.[46] We hypothesize that this might be caused by post-mating incompatibilities, which could be associated with signaling processes involved in sexual reproduction. This is supported by our unsuccessful attempts to restore teliospore formation by overexpressing the *U. maydis* TF *ros1* in rUSH, which was shown to be crucial for karyogamy and matrix formation[42] (data not shown). To overcome post-mating barriers and obtain teliospores in rUSH, future approaches might include the overexpression of TFs that are highly induced during the reproductive phase and involved in the regulation of developmental genes essential for sporogenesis.

U. maydis lacks an RNAi machinery, which is a distinctive feature among the smuts.[15] The substantial role of the RNAi

machinery in the observed downregulation of *U. maydis* effector genes in rUSH was refuted, as mating with the *S. reilianum* dicer gene deletion mutant did not alter the expression levels. Except for the RNAi, natural antisense transcripts (NATs) might play a role in regulating gene expression in rUSH.[47] In future research, the potential impact of NATs on rUSH should be investigated. After the so-called "transcriptomic shock" that often follows the fusion of different genomes,[1] RNA-seq of rUSH-infected maize leaves revealed 253 differentially expressed one-to-one effector orthologs, including rUSH-specific expression of effector genes. These particular expression patterns are most likely the result of an interaction between *cis*- and *trans*-regulation, which differs from earlier studies on interspecific hybrids where gene expression was either equally or more strongly affected by *cis*-regulation compared to *trans*-regulation.[48,49] Consistent with our results, hybrid-specific expression has also been observed in yeast hybrids, although to a lesser degree than what was noted in rUSH.[50] The effector gene *Umtin2* was differentially expressed between the species and within rUSH, which is in line with a previous study.[5] The variation in *tin2* expression is most likely to be due to *cis*-regulatory elements in the promoter region, which play a crucial role in determining the different expression levels between species.

Effector gene expression in *U. maydis* is tightly regulated in a spatiotemporal manner by a hierarchical network of TFs.[11,43,51,52] When *Umhdp2* was overexpressed in rUSH, the formation of leaf tumors was observed in all infected maize seedlings. This identifies Hdp2 as a key regulator of tumorigenesis-associated effector genes. Using rUSH as a platform, future work involving consecutive knockout mutants and parallel overexpression of tumor-inducing effector genes will help to unravel a minimal key set of effectors required for the induction of plant tumors. Taken together, the results show that the generation of a recombinant, interspecific hybrid disclosed the regulatory patterns of effector orthologs in *U. maydis* and *S. reilianum*. The characterization of rUSH facilitated the identification of new virulence factors in both *U. maydis* and *S. reilianum* and highlighted maize genes that may play a role in the tumor pathways initiated by *U. maydis* infections. This study makes an important contribution to understanding how the genetic interplay between different species influences virulence and disease progression in plant pathogens. Above all, however, the establishment of rUSH is a significant milestone in the mechanistic elucidation of the genetic basis of fungal tumor formation in plants.

Limitations of the study

A limitation of the study is our unsuccessful attempts to obtain teliospores in either rUSH or rUSH_OE_*Umhdp2*. Future experiments should aim to elucidate unknown elements that contribute to putative post-mating incompatibilities in rUSH and elements that influence the completion of the life cycle, i.e., epigenetic factors or mito-nuclear interactions, which were not addressed in this study. Furthermore, a comparison of tumor formation on maize seedlings of WT *U. maydis* with rUSH_OE_*Umhdp2* may provide insights into the tumor cell type and might help to further elucidate the regulation of cell-type-specific effectors and the time point at which further tumor development is blocked in rUSH_OE_*Umhdp2*.

RESOURCE AVAILABILITY

Lead contact

Requests for additional information and resources should be directed to and will be fulfilled by the lead contact, Gunther Doehlemann (g.doehlemann@uni-koeln.de).

Materials availability

Source data are provided in this paper. Strains, plasmids, and all data supporting the findings of this study that are not directly available within the paper (and its supplemental information) will be made available upon request from the corresponding authors (G.D. and J.W.).

Data and code availability

Raw data of RNA-seq analyses are publicly accessible in the NCBI Gene Expression Omnibus (accession numbers GEO: GSE292562 [*S. reilianum*-, *U. maydis*-, and rUSH-infected maize leaves at 20 hpi, 3 dpi, and 6 dpi] and GSE293102 [rUSH-, FB1xSRZ2-, and rUSH_OE_*Umhdp2*-infected maize leaves at 3 dpi]). Any additional information needed to reanalyze the data reported in this paper is available upon request from the lead contact.

ACKNOWLEDGMENTS

This project has received funding from the European Research Council (ERC) under the European Union's Horizon 2020 research and innovation program (grant agreement no. 771035), as well as from the Cluster of Excellence on Plant Sciences (CEPLAS) funded under Germany's Excellence Strategy—EXC 2048/1—project ID: 390686111.

AUTHOR CONTRIBUTIONS

G.D. and W.Z. supervised the project. G.D., W.Z., and J.W. designed the experiments. J.W. and W.Z. conducted the experiments. T.W. generated FB1_*Sra1b1*. J.W. wrote the manuscript with contributions from all authors.

DECLARATION OF INTERESTS

The authors declare no competing interests.

STAR★METHODS

Detailed methods are provided in the online version of this paper and include the following:

- KEY RESOURCES TABLE
- METHOD DETAILS
  - Fungal strains and growth conditions
  - Plant infections
  - Staining and microscopy
  - DNA and RNA preparation
  - qRT-PCR
- QUANTIFICATION AND STATISTICAL ANALYSIS
  - RNA-sequencing data analysis
  - Statistical analysis

SUPPLEMENTAL INFORMATION

Supplemental information can be found online at https://doi.org/10.1016/j.celrep.2025.115772.

Received: February 14, 2025
Revised: April 9, 2025
Accepted: May 12, 2025
Published: June 13, 2025

REFERENCES

1. Steensels, J., Gallone, B., and Verstrepen, K.J. (2021). Interspecific hybridization as a driver of fungal evolution and adaptation. Nat. Rev. Microbiol. *19*, 485–500. https://doi.org/10.1038/s41579-021-00537-4.
2. Hovhannisyan, H., Saus, E., Ksiezopolska, E., and Gabaldón, T. (2020). The Transcriptional Aftermath in Two Independently Formed Hybrids of the Opportunistic Pathogen Candida orthopsilosis. mSphere *5*, e00282-20. https://doi.org/10.1128/msphere.00282-20.
3. Stukenbrock, E.H. (2016). The role of hybridization in the evolution and emergence of new fungal plant pathogens. Phytopathology *106*, 104–112. https://doi.org/10.1094/PHYTO-08-15-0184-RVW.
4. Combes, M.C., Hueber, Y., Dereeper, A., Rialle, S., Herrera, J.C., and Lashermes, P. (2015). Regulatory divergence between parental alleles determines gene expression patterns in hybrids. Genome Biol. Evol. *7*, 1110–1121. https://doi.org/10.1093/gbe/evv057.
5. Zuo, W., Depotter, J.R.L., Gupta, D.K., Thines, M., and Doehlemann, G. (2021). Cross-species analysis between the maize smut fungi *Ustilago maydis* and *Sporisorium reilianum* highlights the role of transcriptional change of effector orthologs for virulence and disease. New Phytol. *232*, 719–733. https://doi.org/10.1111/nph.17625.
6. Ghareeb, H., Drechsler, F., Löfke, C., Teichmann, T., and Schirawski, J. (2015). SUPPRESSOR OF APICAL DOMINANCE1 of *Sporisorium reilianum* modulates inflorescence branching architecture in maize and Arabidopsis. Plant Physiol. *169*, 2789–2804. https://doi.org/10.1104/pp.15.01347.
7. Ghareeb, H., Becker, A., Iven, T., Feussner, I., and Schirawski, J. (2011). *Sporisorium reilianum* infection changes inflorescence and branching architectures of maize. Plant Physiol. *156*, 2037–2052. https://doi.org/10.1104/pp.111.179499.
8. Brefort, T., Doehlemann, G., Mendoza-Mendoza, A., Reissmann, S., Djamei, A., and Kahmann, R. (2009). *Ustilago maydis* as a pathogen. Annu. Rev. Phytopathol. *47*, 423–445. https://doi.org/10.1146/annurev-phyto-080508-081923.
9. Schulz (1990). Erratum: The b alleles of *U. maydis*, whose combinations program pathogenic development, code for polypeptides containing a homeodomain-related motif. Cell *60*, 521.
10. Gillissen, B., Bergemann, J., Sandmann, C., Schroeer, B., Bölker, M., and Kahmann, R. (1992). A two-component regulatory system for self/non-self recognition in *Ustilago maydis*. Cell *68*, 647–657. https://doi.org/10.1016/0092-8674(92)90141-X.
11. Heimel, K., Scherer, M., Vranes, M., Wahl, R., Pothiratana, C., Schuler, D., Vincon, V., Finkernagel, F., Flor-Parra, I., and Kämper, J. (2010). The transcription factor Rbf1 is the master regulator for b-mating type controlled pathogenic development in *Ustilago maydis*. PLoS Pathog. *6*, e1001035. https://doi.org/10.1371/journal.ppat.1001035.
12. Flor-Parra, I., Vranes, M., Kämper, J., and Pérez-Martín, J. (2006). Biz1, a zinc finger protein required for plant invasion by *Ustilago maydis*, regulates the levels of a mitotic cyclin. Plant Cell *18*, 2369–2387. https://doi.org/10.1105/tpc.106.042754.
13. Lanver, D., Berndt, P., Tollot, M., Naik, V., Vranes, M., Warmann, T., Münch, K., Rössel, N., and Kahmann, R. (2014). Plant Surface Cues Prime *Ustilago maydis* for Biotrophic Development. PLoS Pathog. *10*, e1004272. https://doi.org/10.1371/journal.ppat.1004272.
14. Lanver, D., Tollot, M., Schweizer, G., Lo Presti, L., Reissmann, S., Ma, L.S., Schuster, M., Tanaka, S., Liang, L., Ludwig, N., and Kahmann, R. (2017). *Ustilago maydis* effectors and their impact on virulence. Nat. Rev. Microbiol. *15*, 409–421. https://doi.org/10.1038/nrmicro.2017.33.
15. Schirawski, J., Mannhaupt, G., Münch, K., Brefort, T., Schipper, K., Doehlemann, G., Di Stasio, M., Rössel, N., Mendoza-Mendoza, A., and Pester, D. (2010). Pathogenicity determinants in smut fungi revealed by genome comparison. Science *330*, 1546–1548. https://doi.org/10.1126/science.1195330.
16. Kämper, J., Kahmann, R., Bölker, M., Ma, L.J., Brefort, T., Saville, B.J., Banuett, F., Kronstad, J.W., Gold, S.E., Müller, O., et al. (2006). Insights from the genome of the biotrophic fungal plant pathogen *Ustilago maydis*. Nature *444*, 97–101. https://doi.org/10.1038/nature05248.
17. Brefort, T., Tanaka, S., Neidig, N., Doehlemann, G., Vincon, V., and Kahmann, R. (2014). Characterization of the Largest Effector Gene Cluster of *Ustilago maydis*. PLoS Pathog. *10*, e1003866. https://doi.org/10.1371/journal.ppat.1003866.
18. Ghareeb, H., Zhao, Y., and Schirawski, J. (2019). *Sporisorium reilianum* possesses a pool of effector proteins that modulate virulence on maize. Mol. Plant Pathol. *20*, 124–136. https://doi.org/10.1111/mpp.12744.
19. Shi, W., Stolze, S.C., Nakagami, H., Misas Villamil, J.C., Saur, I.M.L., and Doehlemann, G. (2023). Combination of in vivo proximity labeling and co-immunoprecipitation identifies the host target network of a tumor-inducing effector in the fungal maize pathogen *Ustilago maydis*. J. Exp. Bot. *74*, 4736–4750. https://doi.org/10.1093/jxb/erad188.
20. Redkar, A., Hoser, R., Schilling, L., Zechmann, B., Krzymowska, M., Walbot, V., and Doehlemann, G. (2015). A secreted effector protein of *Ustilago maydis* guides maize leaf cells to form tumors. Plant Cell *27*, 1332–1351. https://doi.org/10.1105/tpc.114.131086.
21. Hemetsberger, C., Mueller, A.N., Matei, A., Herrberger, C., Hensel, G., Kumlehn, J., Mishra, B., Sharma, R., Thines, M., Hückelhoven, R., and Doehlemann, G. (2015). The fungal core effector Pep1 is conserved across smuts of dicots and monocots. New Phytol. *206*, 1116–1126. https://doi.org/10.1111/nph.13304.
22. Stirnberg, A., and Djamei, A. (2016). Characterization of ApB73, a virulence factor important for colonization of *Zea mays* by the smut *Ustilago maydis*. Mol. Plant Pathol. *17*, 1467–1479. https://doi.org/10.1111/mpp.12442.
23. Ma, L.S., Wang, L., Trippel, C., Mendoza-Mendoza, A., Ullmann, S., Moretti, M., Carsten, A., Kahnt, J., Reissmann, S., Zechmann, B., et al. (2018). The *Ustilago maydis* repetitive effector Rsp3 blocks the antifungal activity of mannose-binding maize proteins. Nat. Commun. *9*, 1711. https://doi.org/10.1038/s41467-018-04149-0.
24. Tanaka, S., Schweizer, G., Rössel, N., Fukada, F., Thines, M., and Kahmann, R. (2019). Neofunctionalization of the secreted Tin2 effector in the fungal pathogen *Ustilago maydis*. Nat. Microbiol. *4*, 251–257. https://doi.org/10.1038/s41564-018-0304-6.
25. Zuo, W., Depotter, J.R.L., Stolze, S.C., Nakagami, H., and Doehlemann, G. (2023). A transcriptional activator effector of *Ustilago maydis* regulates hyperplasia in maize during pathogen-induced tumor formation. Nat. Commun. *14*, 6722. https://doi.org/10.1038/s41467-023-42522-w.
26. Kellner, R., Vollmeister, E., Feldbrügge, M., and Begerow, D. (2011). Interspecific sex in grass smuts and the genetic diversity of their pheromone-receptor system. PLoS Genet. *7*, e1002436. https://doi.org/10.1371/journal.pgen.1002436.
27. Schirawski, J., Heinze, B., Wagenknecht, M., and Kahmann, R. (2005). Mating type loci of *Sporisorium reilianum*: Novel pattern with three a and multiple b specificities. Eukaryot. Cell *4*, 1317–1327. https://doi.org/10.1128/EC.4.8.1317-1327.2005.
28. Bosch, J., Czedik-Eysenberg, A., Hastreiter, M., Khan, M., Güldener, U., and Djamei, A. (2019). Two is better than one: Studying *Ustilago bromivora-Brachypodium* compatibility by using a hybrid pathogen. Mol. Plant Microbe Interact. *32*, 1623–1634. https://doi.org/10.1094/MPMI-05-19-0148-R.
29. Storfie, E.R.M., and Saville, B.J. (2021). Fungal Pathogen Emergence: Investigations with an *Ustilago maydis* × *Sporisorium reilianum* Hybrid. J. Fungi *7*, 672.
30. Day, P.R., and Anagnostakis, S.L. (1971). Corn Smut Dikaryon in Culture. Nat. New Biol. *231*, 19–20.
31. Djamei, A., Schipper, K., Rabe, F., Ghosh, A., Vincon, V., Kahnt, J., Osorio, S., Tohge, T., Fernie, A.R., Feussner, I., et al. (2011). Metabolic priming by a secreted fungal effector. Nature *478*, 395–398. https://doi.org/10.1038/nature10454.

32. Mueller, A.N., Ziemann, S., Treitschke, S., Aßmann, D., and Doehlemann, G. (2013). Compatibility in the *Ustilago maydis*-Maize Interaction Requires Inhibition of Host Cysteine Proteases by the Fungal Effector Pit2. PLoS Pathog. *9*, e1003177. https://doi.org/10.1371/journal.ppat.1003177.

33. Misas Villamil, J.C., Mueller, A.N., Demir, F., Meyer, U., Ökmen, B., Schulze Hüynck, J., Breuer, M., Dauben, H., Win, J., Huesgen, P.F., and Doehlemann, G. (2019). A fungal substrate mimicking molecule suppresses plant immunity via an inter-kingdom conserved motif. Nat. Commun. *10*, 1576. https://doi.org/10.1038/s41467-019-09472-8.

34. Ludwig, N., Reissmann, S., Schipper, K., Gonzalez, C., Assmann, D., Glatter, T., Moretti, M., Ma, L.S., Rexer, K.H., Snetselaar, K., and Kahmann, R. (2021). A cell surface-exposed protein complex with an essential virulence function in *Ustilago maydis*. Nat. Microbiol. *6*, 722–730. https://doi.org/10.1038/s41564-021-00896-x.

35. Tanaka, S., Brefort, T., Neidig, N., Djamei, A., Kahnt, J., Vermerris, W., Koenig, S., Feussner, K., Feussner, I., and Kahmann, R. (2014). A secreted *Ustilago maydis* effector promotes virulence by targeting anthocyanin biosynthesis in maize. eLife *3*, e01355. https://doi.org/10.7554/elife.01355.

36. Bindics, J., Khan, M., Uhse, S., Kogelmann, B., Baggely, L., Reumann, D., Ingole, K.D., Stirnberg, A., Rybecky, A., Darino, M., et al. (2022). Many ways to TOPLESS – manipulation of plant auxin signalling by a cluster of fungal effectors. New Phytol. *236*, 1455–1470. https://doi.org/10.1111/nph.18315.

37. Huang, L., Ökmen, B., Stolze, S.C., Kastl, M., Khan, M., Hilbig, D., Nakagami, H., Djamei, A., and Doehlemann, G. (2024). The fungal pathogen *Ustilago maydis* targets the maize corepressor RELK2 to modulate host transcription for tumorigenesis. New Phytol. *241*, 1747–1762. https://doi.org/10.1111/nph.19448.

38. Doehlemann, G., Van Der Linde, K., Aßmann, D., Schwammbach, D., Hof, A., Mohanty, A., Jackson, D., and Kahmann, R. (2009). Pep1, a secreted effector protein of *Ustilago maydis*, is required for successful invasion of plant cells. PLoS Pathog. *5*, e1000290. https://doi.org/10.1371/journal.ppat.1000290.

39. Khan, M., Uhse, S., Bindics, J., Kogelmann, B., Nagarajan, N., Tabassum, R., Ingole, K.D., and Djamei, A. (2024). Tip of the iceberg? Three novel TOPLESS-interacting effectors of the gall-inducing fungus *Ustilago maydis*. New Phytol. *244*, 949–961. https://doi.org/10.1111/nph.19967.

40. Lin, J.S., Happel, P., and Kahmann, R. (2021). Nuclear status and leaf tumor formation in the *Ustilago maydis*–maize pathosystem. New Phytol. *231*, 399–415. https://doi.org/10.1111/nph.17377.

41. Zahiri, A., Heimel, K., Wahl, R., Rath, M., and Kämper, J. (2010). The *Ustilago maydis* forkhead transcription factor Fox1 is involved in the regulation of genes required for the attenuation of plant defenses during pathogenic development. Mol. Plant Microbe Interact. *23*, 1118–1129. https://doi.org/10.1094/MPMI-23-9-1118.

42. Tollot, M., Assmann, D., Becker, C., Altmüller, J., Dutheil, J.Y., Wegner, C. E., and Kahmann, R. (2016). The WOPR Protein Ros1 Is a Master Regulator of Sporogenesis and Late Effector Gene Expression in the Maize Pathogen *Ustilago maydis*. PLoS Pathog. *12*, e1005697. https://doi.org/10.1371/journal.ppat.1005697.

43. Lanver, D., Müller, A.N., Happel, P., Schweizer, G., Haas, F.B., Franitza, M., Pellegrin, C., Reissmann, S., Altmüller, J., Rensing, S.A., and Kahmann, R. (2018). The biotrophic development of *Ustilago maydis* studied by RNA-seq analysis. Plant Cell *30*, 300–323. https://doi.org/10.1105/tpc.17.00764.

44. Doehlemann, G., Wahl, R., Horst, R.J., Voll, L.M., Usadel, B., Poree, F., Stitt, M., Pons-Kühnemann, J., Sonnewald, U., Kahmann, R., and Kämper, J. (2008). Reprogramming a maize plant: Transcriptional and metabolic changes induced by the fungal biotroph Ustilago maydis. Plant J. *56*, 181–195. https://doi.org/10.1111/j.1365-313X.2008.03590.x.

45. Heinze, B. (2009). Comparative Analysis of the Maize Smut Fungi. Ustilago maydis and Sporisorium reilianum. https://doi.org/10.17192/z2010.0093.

46. Samarasinghe, H., You, M., Jenkinson, T.S., Xu, J., and James, T.Y. (2020). Hybridization Facilitates Adaptive Evolution in Two Major Fungal Pathogens. Genes *11*, 101.

47. Donaldson, M.E., and Saville, B.J. (2013). *Ustilago maydis* natural antisense transcript expression alters mRNA stability and pathogenesis. Mol. Microbiol. *89*, 29–51. https://doi.org/10.1111/mmi.12254.

48. Hill, M.S., Vande Zande, P., and Wittkopp, P.J. (2021). Molecular and evolutionary processes generating variation in gene expression. Nat. Rev. Genet. *22*, 203–215. https://doi.org/10.1038/s41576-020-00304-w.

49. Runemark, A., Moore, E.C., and Larson, E.L. (2024). Hybridization and gene expression: Beyond differentially expressed genes. Mol. Ecol., e17303. https://doi.org/10.1111/mec.17303.

50. Tirosh, I., Reikhav, S., Levy, A.A., and Barkai, N. (2009). A yeast hybrid provides insight into the evolution of gene expression regulation. Science *324*, 659–662. https://doi.org/10.1126/science.1169766.

51. Feldbrügge, M., Kämper, J., Steinberg, G., and Kahmann, R. (2004). Regulation of mating and pathogenic development in *Ustilago maydis*. Curr. Opin. Microbiol. *7*, 666–672. https://doi.org/10.1016/j.mib.2004.10.006.

52. Skibbe, D.S., Doehlemann, G., Fernandes, J., and Walbot, V. (2010). Maize Tumors Caused by *Ustilago maydis* Require Organ-Specific Genes in Host and Pathogen. Science *328*, 89–92.

53. Schuster, M., Schweizer, G., Reissmann, S., and Kahmann, R. (2016). Genome editing in *Ustilago maydis* using the CRISPR-Cas system. Fungal Genet. Biol. *89*, 3–9. https://doi.org/10.1016/j.fgb.2015.09.001.

54. Zuo, W., Depotter, J.R., and Doehlemann, G. (2020). Cas9HF1 enhanced specificity in *Ustilago maydis*. Fungal Biol. *124*, 228–234. https://doi.org/10.1016/j.funbio.2020.02.006.

55. Werner, J., Zuo, W., and Doehlemann, G. (2024). CRISPR/Cas9 Ribonucleoprotein- Mediated Mutagenesis in Sporisorium reilianum. Bio Protoc *14*, 1–10. https://doi.org/10.21769/BioProtoc.4978.2.

56. Redkar, A., and Doehlemann, G. (2016). *Ustilago maydis* Virulence Assays in Maize. Bio. Protoc. *6*, 1–7. https://doi.org/10.21769/BioProtoc.1760.

57. Bolger, A.M., Lohse, M., and Usadel, B. (2014). Trimmomatic: A flexible trimmer for Illumina sequence data. Bioinformatics *30*, 2114–2120. https://doi.org/10.1093/bioinformatics/btu170.

58. Langmead, B., and Salzberg, S.L. (2012). Fast gapped-read alignment with Bowtie 2. Nat. Methods *9*, 357–359. https://doi.org/10.1038/nmeth.1923.

59. Anders, S., Pyl, P.T., and Huber, W. (2015). HTSeq-A Python framework to work with high-throughput sequencing data. Bioinformatics *31*, 166–169. https://doi.org/10.1093/bioinformatics/btu638.

STAR★METHODS

KEY RESOURCES TABLE

REAGENT or RESOURCE	SOURCE	IDENTIFIER
Deposited data		
Raw and analyzed data	This paper	GEO: GSE292562* and GSE29310*
Zea mays reference genome	Maize GDB	https://www.maizegdb.org/genome/assembly/Zm-B73-REFERENCE-NAM-5.0
Ustilago maydis reference genome	Kämper et al., 2006	N/A
Sporisorium reilianum reference genome	Schirawski et al., 2010	N/A
Experimental models: Organisms/strains		
FB1	Banuett & Herskowitz, 1989	N/A
FB2	Banuett & Herskowitz, 1989	N/A
SG200	Bölker et al., 1995, Kämper et al., 2006	N/A
FB1_*Sra1b1*	This paper	N/A
FB1_*Sra1b1*_psr10057_*UMAG_05302*_#3	This paper	N/A
FB1:CR-*UMAG_00533* #1 FB1:CR-*UMAG_00533* #2 FB1:CR-*UMAG_00533* #8 FB2:CR-*UMAG_00533* #1 FB2:CR-*UMAG_00533* #2 FB2:CR-*UMAG_00533* #4	This paper	N/A
FB1:CR-*UMAG_02462* #2 FB1:CR-*UMAG_02462* #4 FB1:CR-*UMAG_02462* #5 FB2:CR-*UMAG_02462* #1 FB2:CR-*UMAG_02462* #2	This paper	N/A
FB1:CR-*UMAG_04242* #2 FB1:CR-*UMAG_04242* #3 FB2:CR-*UMAG_04242* #3 FB2:CR-*UMAG_04242* #5 FB2:CR-*UMAG_04242* #8	This paper	N/A
SG200:CR-*UMAG_06257* #1 SG200:CR-*UMAG_06257* #7 SG200:CR-*UMAG_06257* #8	This paper	N/A
SG200:CR-*UMAG_10256* #6 SG200:CR-*UMAG_10256* #13 SG200:CR-*UMAG_10256* #16	This paper	N/A
SG200:CR-*UMAG_05312* #1 SG200:CR-*UMAG_05312* #3 SG200:CR-*UMAG_05312* #4	This paper	N/A
SG200:CR-*UMAG_10553* #1 SG200:CR-*UMAG_10553* #2 SG200:CR-*UMAG_10553* #8	This paper	N/A
SRZ1	Schirawski et al., 2010	N/A
SRZ2	Schirawski et al., 2010	N/A
SRZ2_Δ*sr16838*_#7	This paper	N/A
SRZ2_Δ*sr16838*_#15	This paper	N/A
SRZ1Δ*sr16075* #3 SRZ1Δ*sr16075* #14 SRZ2Δ*sr16075* #3 SRZ2Δ*sr16075* #5	This paper	N/A

(*Continued on next page*)

Continued

REAGENT or RESOURCE	SOURCE	IDENTIFIER
Oligonucleotides		
Primers used for Cloning, qRT-PCR and sgRNA synthesis, see Table S11	This paper	N/A
Recombinant DNA		
pAGMBII1311_SRZ1_Uma1_#3	This paper	N/A
pAGMBII1311_SRZ1_Umb1_#4	This paper	N/A
pAGM1311_SRZ2_psr10057_UMAG05302_cds#6	This paper	N/A
pAGM1311_FB1_psr10057_UMAG_05302_prom#1	This paper	N/A
p123_proCmu1_*fox1*_2xHA #1	This paper	N/A
p123_proCmu1_*rbf1*_2xHA #2	This paper	N/A
p123_proCmu1_*hdp2*_2xHA #7	This paper	N/A
p123_proCmu1_*ros1*_2xHA	This paper	N/A
p123_proCmu1_*biz1*_2xHA_#3	This paper	N/A
pAGM1311_Δ*sr16075* #1	This paper	N/A
pCas9HF1_*UMAG_06257*	This paper	N/A
pCas9HF1_*UMAG_10256*	This paper	N/A
pCas9HF1_*UMAG_10626*	This paper	N/A
pCas9HF1_*UMAG_05312*	This paper	N/A
pCas9HF1_*UMAG_10553*	This paper	N/A
Software and algorithms		
Trimmomatic software 0.39	Bolger et al., 2014	http://www.usadellab.org/cms/?page=trimmomatic
BOWTIE2 (version 2.3.4.1)	Langmead & Salzberg, 2012	https://bowtie-bio.sourceforge.net/bowtie2/manual.shtml
HTseq-count (version 2.0.4)	Anders et al., 2015	https://htseq.readthedocs.io/en/release_0.11.1/count.html

METHOD DETAILS

Fungal strains and growth conditions

For the RNA-seq analysis and infection studies, the mating compatible strains used, including *U. maydis* (FB1 and FB2), *S. reilianum* (SRZ1xSRZ2), and the recombinant hybrid (rUSH, FB1_*Sra1b1*xSRZ2). Infection assays for effector candidate gene knock-outs (KOs) were carried out using SRZ1 and SRZ2. CRISPR/Cas9 frameshift mutants and knock-in mutants were generated for *U. maydis*[53,54] and *S. reilianum*[55] according to previously established methods. Used oligonucleotides are listed in Table S11. In cases where no donor template was available, CRISPR/Cas9 mutagenesis was implemented as outlined previously.[5] The DNA sequence of the genomic region of interest was sent for sequencing to verify the presence of a premature stop codon. For strains generated through CRISPR/Cas9-assisted homologous recombination (HR), Southern blot analysis was conducted. All strains were cultivated in $YEPS_{light}$ (1% (w/v) yeast extract, 0.4% (w/v) peptone, 0.4% (w/v) sucrose) liquid medium at 28°C with shaking at 200 rpm, or on PDA plates (3.9% (w/v) Potato dextrose agar). For plasmid cloning the *Escherichia coli* strain Top10 was used, grown in dYT liquid medium (1.6% (w/v) tryptone, 1% (w/v) yeast extract, 0.5% (w/v) NaCl) or on YT plates (0.8% (w/v) tryptone, 0.5% (w/v) yeast extract, 0.5% (w/v) NaCl), 1.2% (w/v) Bacto agar), both supplemented with the appropriate antibiotics.

Plant infections

For the infection assays, maize plants were grown under regulated conditions: 16 h of light at 28°C and 8 h of darkness at 22°C. For RNA-seq, *U. maydis*-, *S. reilianum*- and rUSH-infected 7-days old maize seedlings of the cultivar Golden Bantam (demeter) were used. For *S. reilianum* infection assays 7-days old maize seedlings of the cultivar Gaspe Flint (University of Gießen) were infected using a syringe as it was previously shown for *U. maydis*.[56] For infection, a 1:1 mixture of compatible mating partners or the solo-pathogenic strain SG200 was used (OD_{600} of 1). For rUSH infections and microscopy, 0.1% Tween was added prior to infection. The disease symptoms for *U. maydis* were evaluated 12 dpi and for *S. reilianum* 8 wpi.

Staining and microscopy

To observe the formation of appressoria-like structures, 20–22 hpi infected maize leaves were incubated in calcofluor white staining solution (100 μg mL−1; in 0.2 M Tris-HCl; pH 8.0) for 1 min and briefly rinsed with water before observation using the DAPI filter on the

Nikon Eclipse Ti Inverted Microscope.[13] To visualize fungal growth in infected leaves, WGA-AF488 (Wheat Germ Agglutinin, Alexa Fluor 488) and propidium iodide were used to stain fungal and plant cell walls, respectively, as previously described by Doehlemann et al.[38] For microscopy a Nikon Eclipse Ti Inverted Microscope was utilized alongside the Nikon NIS-ELEMENTS software (Düsseldorf, Germany). Images were captured using a HAMAMATSU camera. To visualize fluorescent proteins, the Leica TCS SP8 Confocal Laser Scanning Microscope (Leica, Bensheim, Germany) was employed. GFP was excited at 488 nm and detected within the 490–540 nm range, while mCherry was excited at 561 nm and detected from 580 to 660 nm. The microscopy images were processed using the Leica LAS X.Ink software.

DNA and RNA preparation

Three maize infections were conducted from three independent fungal cultures. 4 cm-long sections (1 cm below the infection side) of the third leaf were collected from at least 12 individual plants. At 20 hpi, ~2 cm-long leaf sections were used and liquid latex was applied to the infected maize leaves, dried, and peeled off for RNA extraction. At the 3 dpi and 6 dpi the plant material was used as described above. The frozen plant tissue and latex were ground into a fine powder using liquid nitrogen. Total RNA was extracted by using TRIzol (Thermo Fisher, Waltham, USA) according to the manufacturer's protocol. Subsequently, a DNase I digest was performed (Thermo Fisher) and the samples were sent to Novogene (UK) for RNA-seq.

qRT-PCR

For qRT-PCR, cDNA was synthesized using RevertAid First Strand cDNA Synthesis kit (Thermo Fisher). The qRT-PCR was performed using a GoTaq qPCR mix (Promega) and a CFX96 Real-Time PCR Detection System (BioRad). DNA extraction of *U. maydis* and *S. reilianum* cultures was prepared using smut lysis buffer (10 mM tris HCl (pH 8.0), 100 mM NaCl, 1 mM Na2-EDTA, 1% SDS, 2% Triton). For biomass quantification, the DNA was isolated using maize extraction buffer (0.1 M Tris-HCl, 0.05 M EDTA, 0.5 M NaCl, 1.5% SDS; after autoclaving addition of 0.3% β-mercaptoethanol) and subsequently purified using a MasterPure Complete DNA and RNA Purification Kit (Epicenter, Madison, USA). For biomass quantification 150 ng of DNA was used. To determine the ratio between fungal *peptidylprolyl isomerase* (*ppi*) and maize *GAPDH* for quantification: $2^{\Delta Ct}$ ($Ct^{ZmGAPDH}$ - Ct^{Umppi}) and for relative gene expression $2^{\Delta Ct}$ (Ct^{Umppi} – Ct^{GOI}) were calculated. For statistical analysis, a student's t-test was conducted. Used oligonucleotides are listed in Table S11.

QUANTIFICATION AND STATISTICAL ANALYSIS

RNA-sequencing data analysis

The RNA-seq was conducted by Novogene. RNA libraries were prepared using an Illumina TruSeq paired-end sequencing (Illumina, SanDiego, CA, USA) performed on a HiSeq4000 platform. Reads of three biological replicates were filtered using the Trimmomatic software[57] 0.39 and standard settings and mapped to a reference assembly using BOWTIE2[58] (version 2.3.4.1). The reference genomes of *U. maydis*[16] and *S. reilianum*[15] were combined before mapping to eliminate a mapping bias to the wrong species. Reads were counted to *U. maydis* and *S. reilianum* using HTseq-count (version 2.0.4).[59] The edgeR package was used for statistical analysis of differential gene expression (counts per million, CPM) and Excel was used to calculate the transcripts per million (TPM) normalized to the different gene lengths between the species. Afterward, one-to-one orthologs were determined.[5] For the comparison between SRZ1xSRZ2 (SR) and FB1xFB2 (UM), the fold change FC(SR/UM) was calculated by dividing the *S. reilianum* transcripts per million (TPM) by *U. maydis* TPM of the wild types. The same analysis was conducted for the orthologous genes in rUSH (Differentially expressed genes: $\log_2FC > 1$ or < -1, $p < 0.05$). Differentially expressed effector genes ($\log_2FC > 1$ or < -1; $p < 0.05$) were grouped using KMeans clustering with one minus Pearson's correlation. The total expression of each ortholog at 3 and 6 dpi was compared between WT and rUSH, leading to the creation of 8 clusters with the following patterns at 6 dpi: C1: higher in SR in WT, higher UM in rUSH (ortholog-specific), C2: no difference in WT, higher in SR in rUSH (ortholog-specific), C3: higher in UM in WT, downregulated in rUSH (*trans*-regulated), C4: higher in SR in WT and rUSH (*cis*-regulated), C5: higher in UM in WT and rUSH (*cis*-regulated), C6: higher in SR in WT, not differentially expressed in rUSH (*trans*-regulated), C7: higher in UM in WT, higher in SR in rUSH (reverse expression), C8: high in SR in WT, higher in SR in rUSH (ortholog-specific expression). ShinyGO v0.66: Gene Ontology Enrichment Analysis + more was used for the GO term enrichment analysis of maize genes upregulated in rUSH_OE_*Umhdp2* vs. rUSH (http://bioinformatics.sdstate.edu/go65/). For details of the used software see key resources table.

Statistical analysis

Data are presented as mean ± SEM. Statistical analysis was performed using Student's t-test (two-tailed) to compare two-group data with normal distribution and equal variance (see Figures 1; 3, 5C, S2 and S4). ANOVA with Tukey's multiple comparisons of different groups was used in Figure 5B. Significance is indicated by asterisks: *, $p < 0.05$; **, $p < 0.01$; ***, $p < 0.001$. Statistical details are provided in the figure legends. N indicates the number of plants used in the corresponding infection assay (Figure 5 and S4).